Supporting Information

Electron redistributed Ni-Co oxide nanoarray as an ORR/OER bifunctional catalyst for low overpotential and long lifespan Li-O_2 batteries

Weiwei Wang,‡[a] Jinyan Cai,‡[a] Hao Wan,[a] Wenlong Cai,[b] Zixuan Zhu,[a] Chengming Wang,[c] Tiansheng Zhou,[a] Zhiguo Hou,*[a] Yongchun Zhu,*[a] and Yitai Qian*[a]

[a]Department of Applied Chemistry
University of Science and Technology of China
Hefei 230026, P. R. China
E-mail: zghou@ustc.edu.cn; ychzhu@ustc.edu.cn; ytqian@ustc.edu.cn

[b]College of Material Science and Engineering
Sichuan University
Chengdu 610000, P. R. China

[c]Instruments Center for Physical Science
University of Science and Technology of China
Hefei 230026, P. R. China

‡ These authors contributed equally to this work.

*Corresponding authors:
E-mail: zghou@ustc.edu.cn; ychzhu@ustc.edu.cn; ytqian@ustc.edu.cn

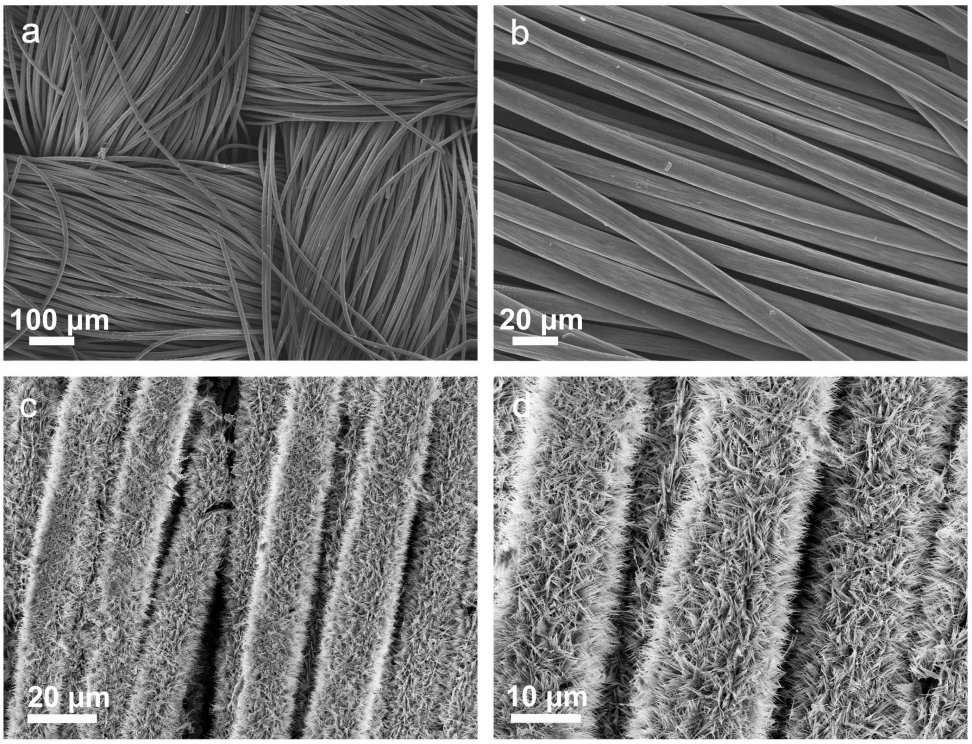

Fig. S1 SEM images of a-b) Carbon Cloth (CC) and c-d) Ni-Co precursor after hydrothermal reaction at 120 ℃ on carbon cloth.

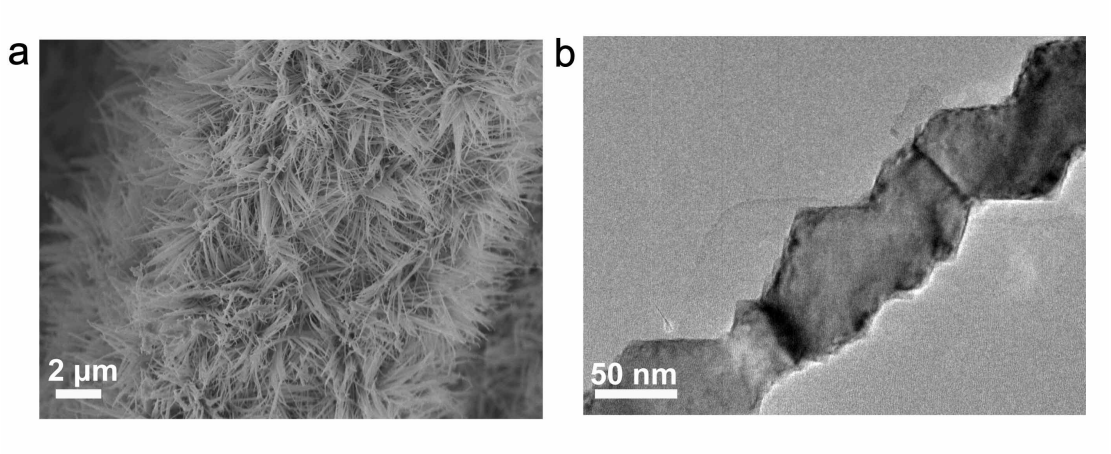

Fig. S2 SEM and TEM images of NCO/CC.

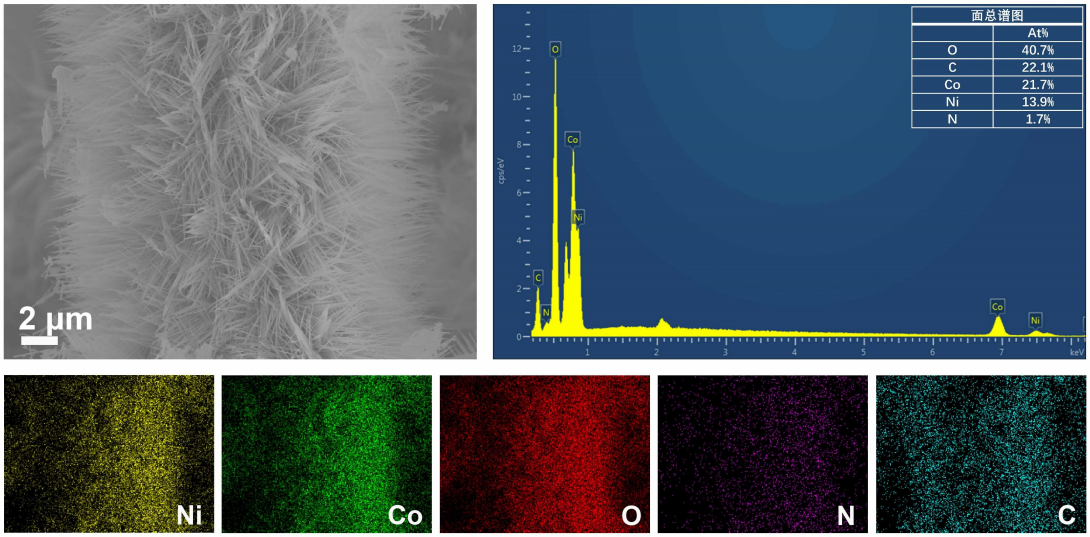

Fig. S3 SEM and Element mappings of NNCO/CC.

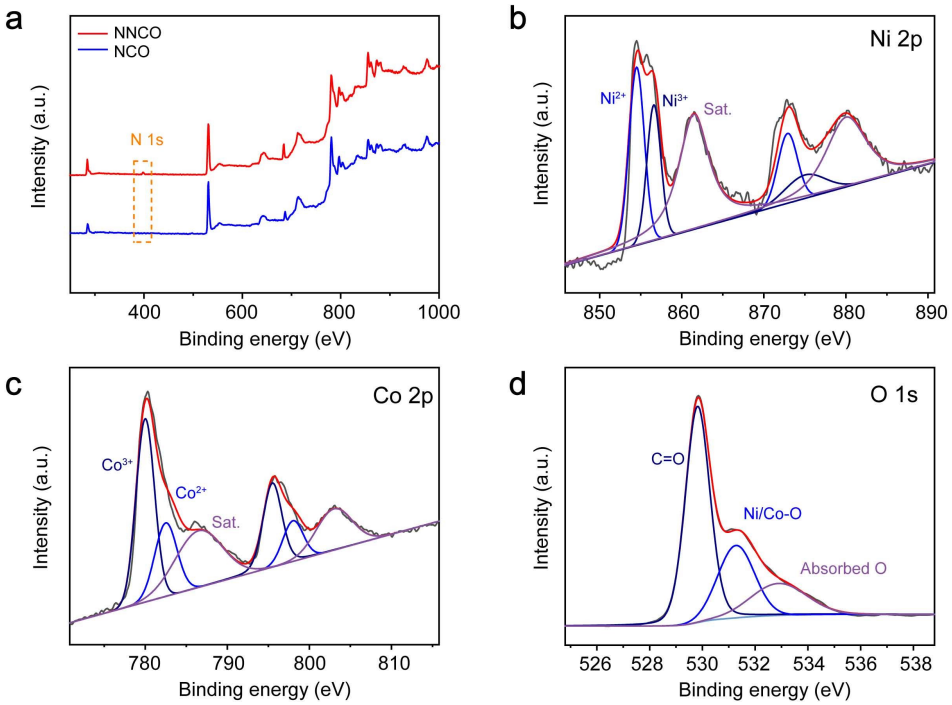

Fig. S4 a) High-resolution XPS spectra of NNCO/CC and NCO/CC; b-d) High-resolution XPS spectra of Ni 2p, Co 2p, and O 1s of NCO/CC.

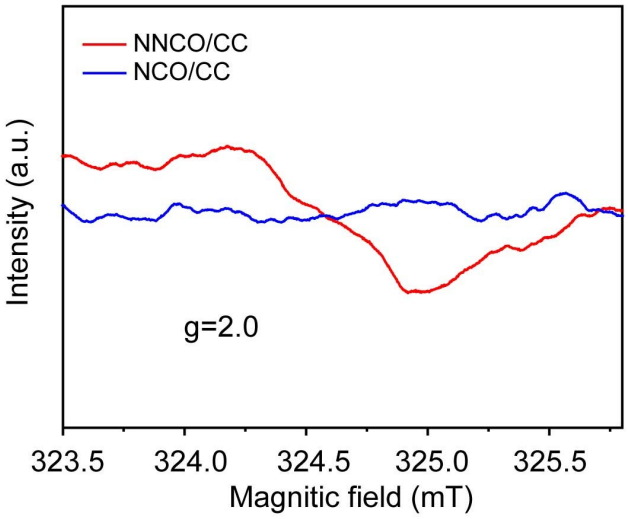

Fig. S5 Electron paramagnetic resonance (EPR) spectra of NNCO and NCO.

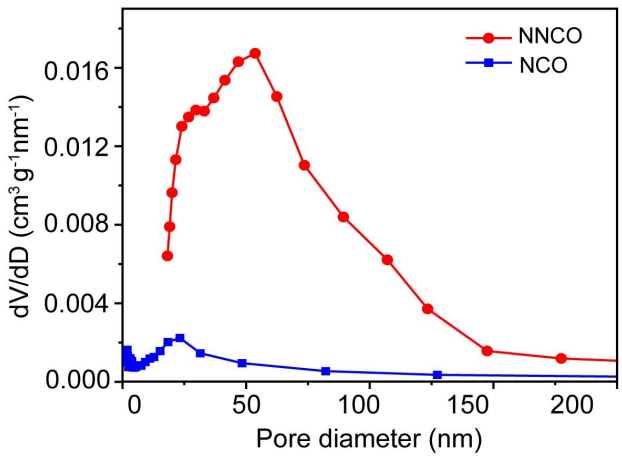

Fig. S6 Pore size distribution curve of NNCO and NCO.

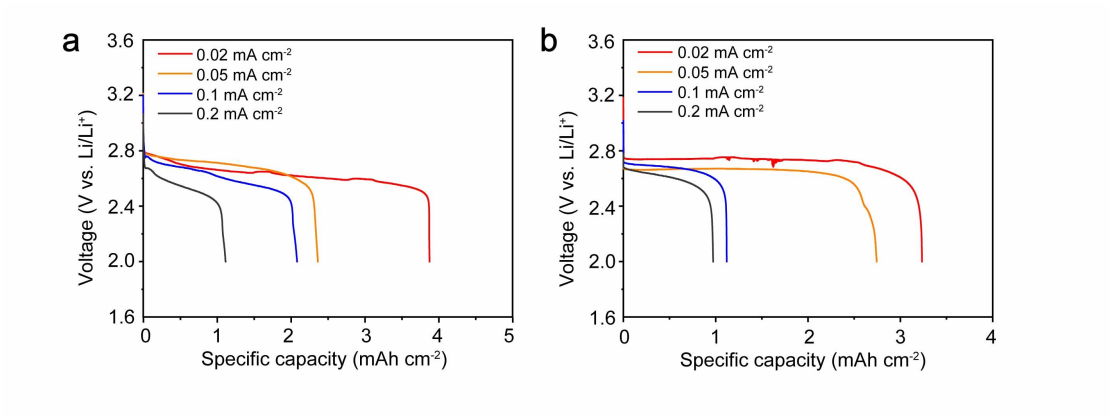

Fig. S7 The rate capability of NCO/CC and KB electrodes with different current densities.

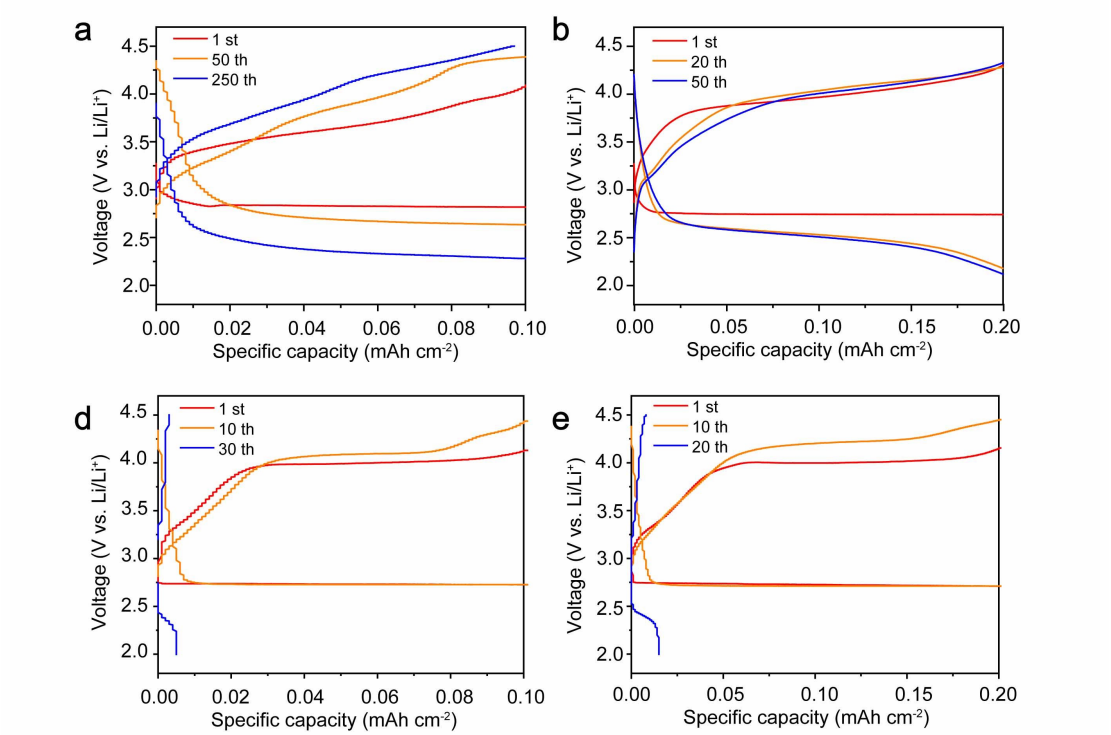

Fig. S8 a-b) Cycling performance of NCO/CC electrode with a capacity restriction (0.1 or 0.2 mAh cm^{-2}) and c-d) Cycling performance of KB electrode with a capacity restriction (0.1 or 0.2 mAh cm^{-2}). The specific capacities are calculated with the areal capacity.

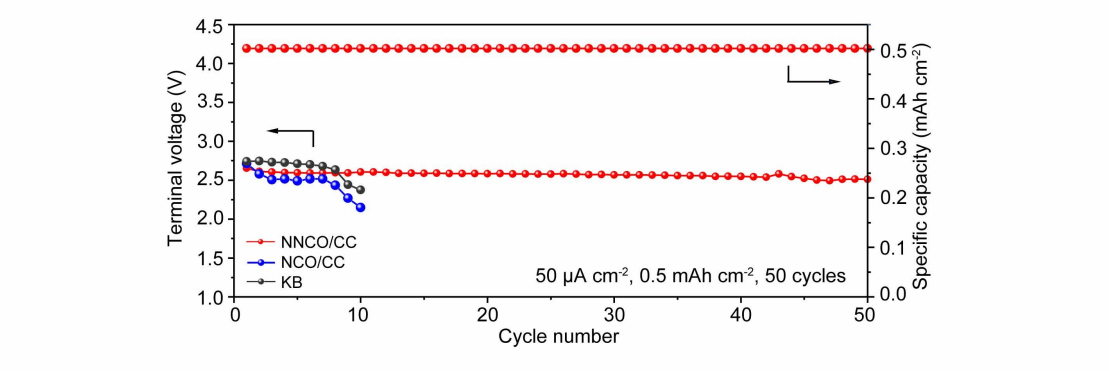

Fig. S9 Cyclic performance of the NNCO/CC, NCO/CC, and KB cathode at a current of 0.05 mA cm^{-2} with a specific capacity limit of 0.5 mAh cm^{-2}.

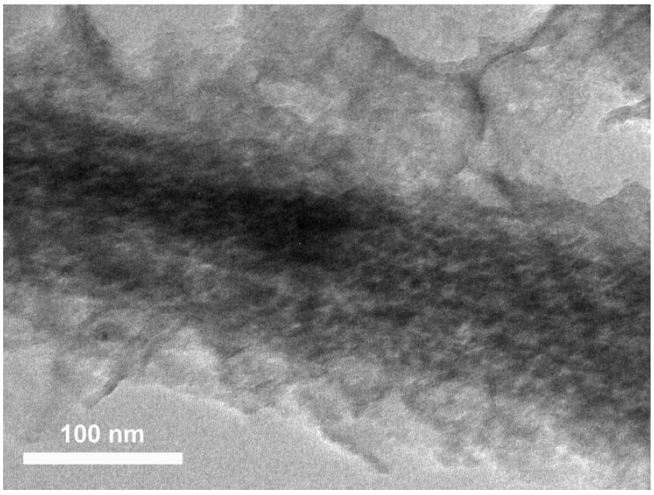

Fig. S10 TEM images of initial discharged containing NNCO/CC electrode.

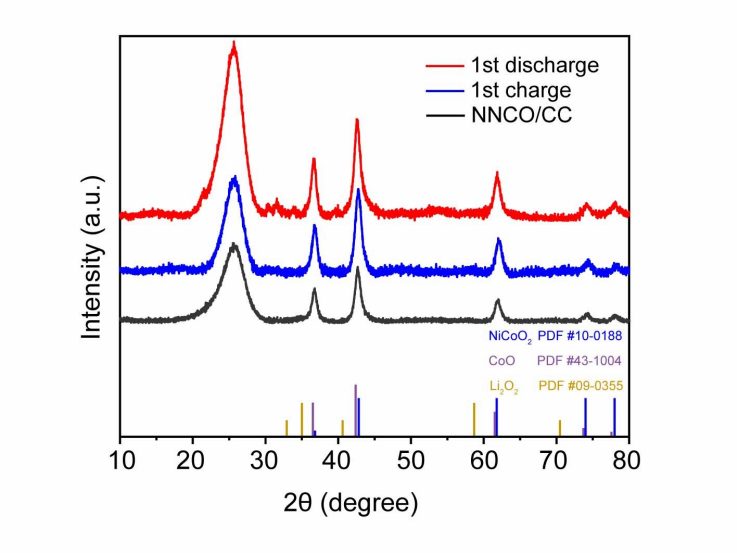

Fig. S11 XRD patterns of NNCO/CC electrode after initial discharging and recharging processes.

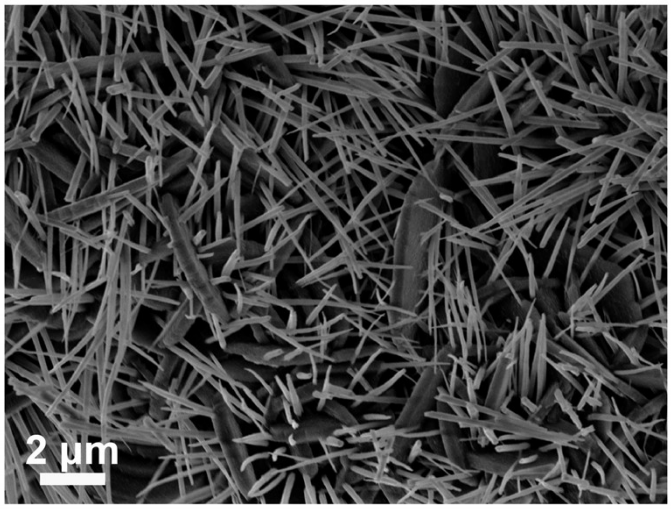

Fig. S12 Ex-situ SEM images of NCO/CC at 0.05 mA cm^{-2} with fully discharged.

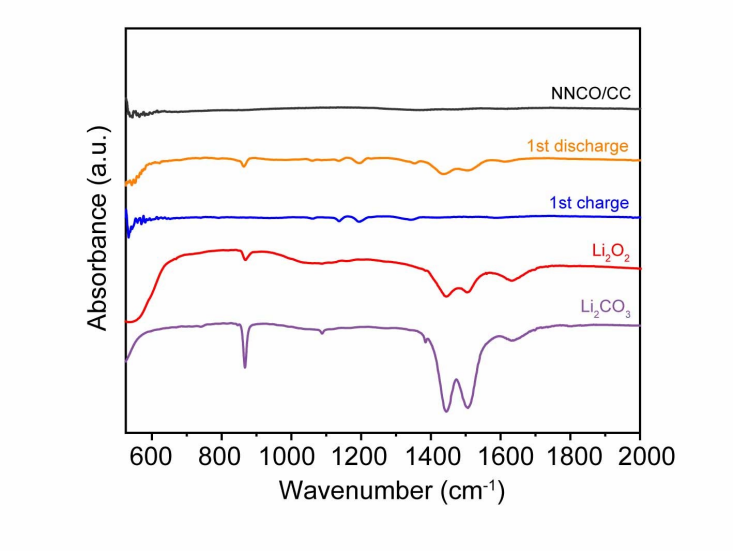

Fig. S13 FTIR spectra for the NNCO/CC at pristine, discharged (0.05 mA cm^{-2}, 0.8 mAh cm^{-2}), and recharged states. Reference materials are also displayed.

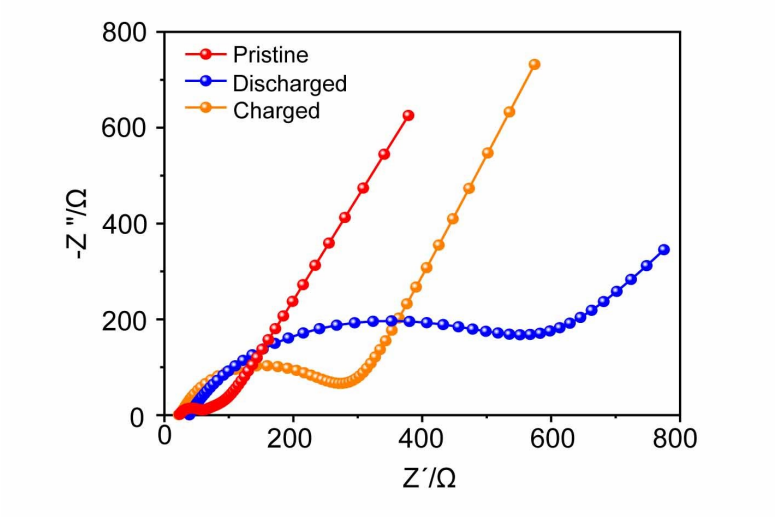

Fig. S14 EIS taken on the NCO/CC cathode at different charging states.

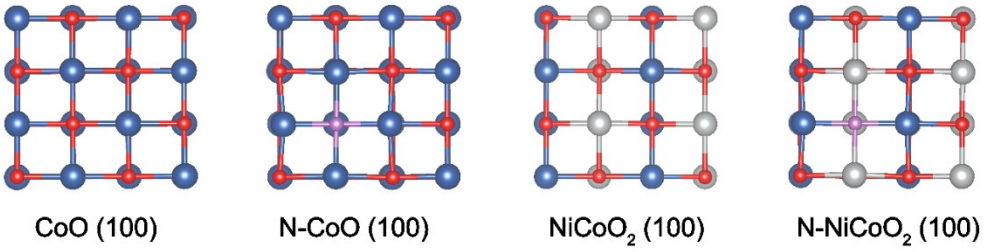

Fig. S15 The top view of CoO, N-CoO, $NiCoO_2$, N-$NiCoO_2$ model.

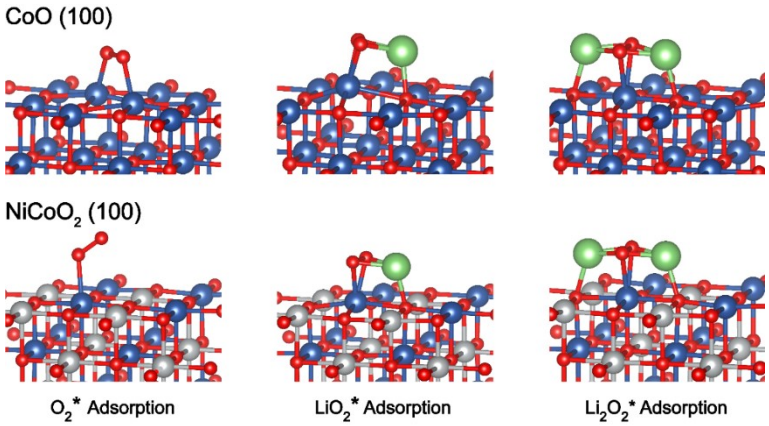

Fig. S16 Optimized structures of different intermediate adsorbed on (100) plane for CoO and $NiCoO_2$.

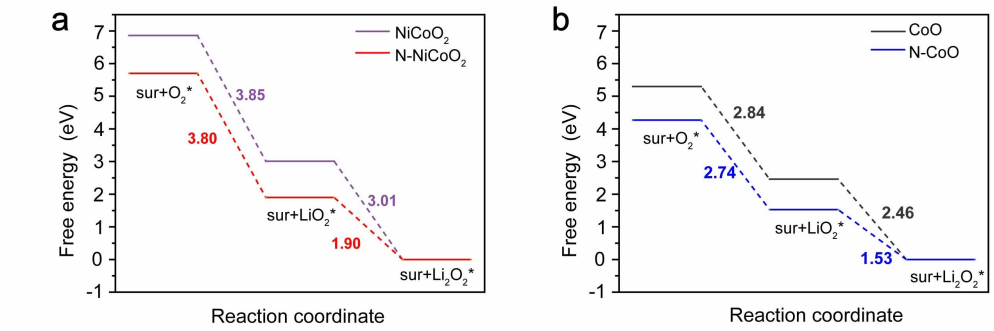

Fig. S17 Calculated free energy diagrams for the discharge-charge reactions on the active surface of CoO, N-CoO, $NiCoO_2$, and N-$NiCoO_2$.

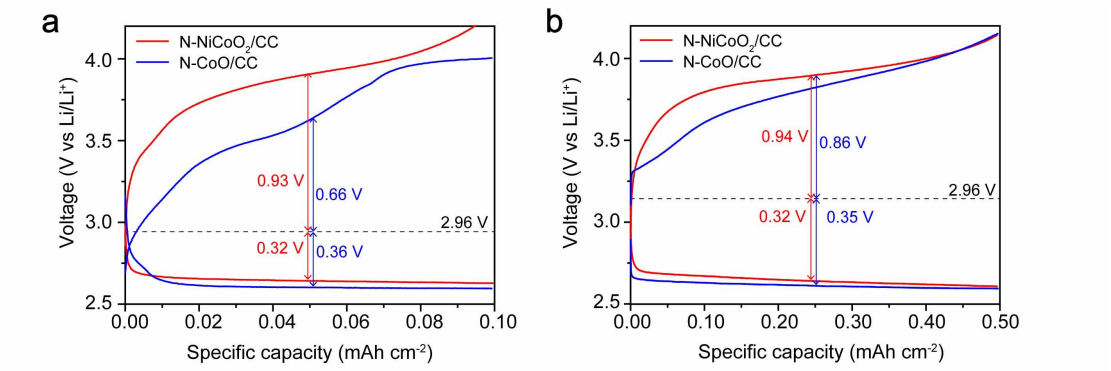

Fig. S18 The initial discharge-charge curves of N-$NiCoO_2$/CC and N-CoO/CC within a current density of 0.05 mA cm^{-2} at a capacity limitation of 0.1 and 0.5 mAh cm^{-2}.

Table S1. ICP of NNCO and NCO.

	Ni (µg/ml)	**Co (µg/ml)**	**Ni:Co**
NNCO	5.653	11.027	0.513
NCO	5.604	11.341	0.494

Table S2. The adsorption energies (ΔE_{ads} [eV]) of LiO_2 and the related factors on the CoO, N-CoO, $NiCoO_2$, and N-$NiCoO_2$.

Catalysts	**Crystal faces**	**d_{Li-O} [Å]**	**d_{O-O} [Å]**	**$\angle_{O-Li-O}$ [°]**	**ΔE_{ads} [eV]**
CoO	(100)	1.833/1.915	1.442	45.182	-1.356
N-CoO	(100)	1.861/1.871	1.45	45.732	-1.313
$NiCoO_2$	(100)	2.103/1.810	1.358	39.739	-0.080
N-$NiCoO_2$	(100)	1.854/1.859	1.39	43.964	-2.605

Table S3. Comparison of electrochemical performance between this work and some reported oxide-based cathodes for LOBs.

Catalysts	**Morphology**	**Overpotential** (V)	**Cycle number** [cycles/current density ($mA \cdot cm^{-2}$)/cutoff capacity (mAh cm^{-2} or mAh g^{-1})]	**Reference**
Co_3O_4-CNF@CC	nanoarrays	0.8	87/0.05/0.15	1
$NiCo_2O_4$/CC	nanowires	0.94	200/0.2/0.3	2
$CoNiO_2$/SCC-N	nanoneedle	~0.5	147/0.05/0.25	3
$Mn_{0.8}Co_{0.2}O$	nanorod	0.48	30/0.05/0.5	4
Fe_2O_3/CNT	nanoparticle	1.3	50/0.1/1.0	5
MoNO	nanosheets	~0.5	50/0.1/1000	6
NNCO/CC	**nanoarrays**	**0.35**	**550/0.05/0.1**	**This work**

Reference

1. L. Xiao, D. Wang, M. Li, B. Deng and J. Liu, *J. Energy Chem.*, 2020, **46**, 248-255.
2. K. Song, B. Yang, Z. Li, Y. Lv, Y. Yu, L. Yuan, X. Shen and X. Hu, *Appl. Surface. Sci.*, 2020, **529**, 147064.
3. H. Liang, F. Chen, M. Zhang, S. Jing, B. Shen, S. Yin and P. Tsiakaras, *Appl. Catal. A: General*, 2019, **574**, 114-121.
4. D. Cao, L. Zheng, Q. Li, J. Zhang, Y. Dong, J. Yue, X. Wang, Y. Bai, G. Tan and C. Wu, *Nano Lett.*, 2021, **21**, 5225-5232.
5. Z. Li, S. Ganapathy, Y. Xu, Q. Zhu, W. Chen, I. Kochetkov, C. George, L. F. Nazar and M. Wagemaker, *Adv. Energy Mater.*, 2018, **8**, 1703513.
6. S. Zhang, G. Wang, J. Jin, L. Zhang and Z. Wen, *Energy Storage Mater.*, 2020, **28**, 342-349.